NEUTRON FLUX MEASUREMENTS AT THE WENDELSTEIN VII-A STELLARATOR

A. Weller, H. Maaßberg

IPP 2/278 October 1985

MAX-PLANCK-INSTITUT FÜR PLASMAPHYSIK

8046 GARCHING BEI MÜNCHEN

MAX-PLANCK-INSTITUT FÜR PLASMAPHYSIK
Garching bei München

NEUTRON FLUX MEASUREMENTS AT THE WENDELSTEIN VII-A STELLARATOR

A. Weller, H. Maaßberg

IPP 2/278 October 1985

Die nachstehende Arbeit wurde im Rahmen des Vertrages zwischen dem Max-Planck-Institut für Plasmaphysik und der Europäischen Atomgemeinschaft über die Zusammenarbeit auf dem Gebiet der Plasmaphysik durchgeführt.

NEUTRON FLUX MEASUREMENTS AT THE WENDELSTEIN VII-A STELLARATOR

A. Weller, H. Maaßberg

Max-Planck-Institut für Plasmaphysik,
Association EURATOM-IPP,
Garching bei München,
Federal Republic of Germany

Abstract

In addition to charge exchange analysis (CX) and charge exchange recombination spectroscopy (CXRS), the time evolution of the central ion temperature during neutral beam heated plasma discharges in the Wendelstein VII-A stellarator is derived from the neutron flux from thermal D-D reactions. In general, good quantitative agreement between the different methods is obtained.

Neutron flux measurements also permit to investigate the slowing down of fast D^+-ions from neutral beam injection (NBI). The results agree well with the predictions based on the assumption of a collisional slowing down mechanism.

CONTENTS

1. Introduction

For typical plasmas in Wendelstein VII-A ($R = 200\ cm$, $a = 10\ cm$, $l = 2$, $m = 5$ helical windings), heated exclusively by neutral beams ($27\ kV$, H^0 or D^0 into a D^+-target plasma, 3-4 beam lines each with a power of $100 - 150\ kW$, almost perpendicular injection (84^o)), ion temperatures in the range $400\ eV \leq T_i \leq 1000\ eV$ are achieved [1,2].

From energy balance considerations [2], in particular a verification of the ion temperatures derived from different experimental methods and also informations about the slowing down of neutral beam particles was requested. Neutron flux measurements contribute to each of the two items: firstly ion temperatures can be derived from the neutron production rate during heating of a D^+ target plasma by H^0 neutral beam injection; secondly slowing down times can be estimated from the transient response and the stationary value of the neutron flux during D^0 injection with an additional neutral beam line, respectively.

2. Ion Temperature from Neutron Flux Measurements

The applied method is described in detail in [3]. Therefore, some informations with respect to the experimental set up and the analysis of the data are added only briefly. A ^3He proportional counter ($10\ atm\ ^3He$, efficiency $\sim 12\ cps/n\ cm^{-2}s^{-1}$) is used to detect the neutrons from the plasma after slowing down in a moderator surrounding the counter tube. The efficieny of the detector was measured with a Pu-Be radioactive neutron source ($\sim 6.5 \cdot 10^6\ n\ s^{-1}$). This source was also moved along the toroidal direction (with fixed position of the detector) in order to derive experimentally the relationship between the measured neutron flux and the (toroidally symmetric) neutron production rate. As in the case of the earlier measurements on ASDEX [3], deviations from the simple quadratic distance law (distance detector-source) occur by neutron shielding and reflection effects.

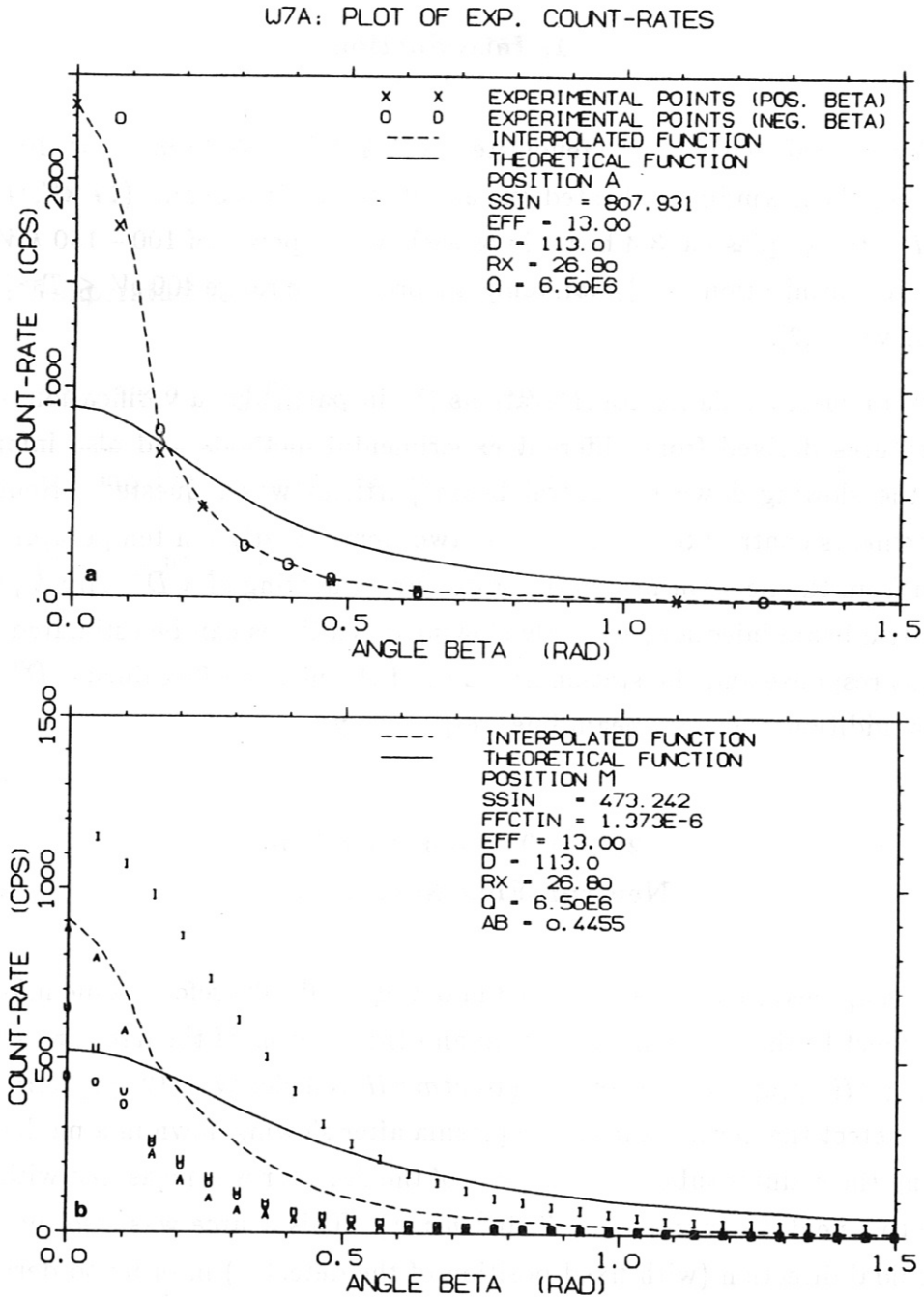

Fig. 1 Dependence of the neutron flux from distance detector-source (source moved toroidally in both directions).

a) Dashed line: fit through measured data. Full line: theoretical curve.

b) Compilation of measurements at four different poloidal positions of the source, extrapolation to position on axis (dashed line) and theoretical curve (full line).

Fig. 1 shows the measured dependency of the signals on the toroidal position of the source with respect to the detector (angle $BETA$ in radians, detector position corresponds to $BETA = 0$). The dashed line in figure 1a is a fit through the measured data. It is much more peaked around the position of the detector as compared to the expected values (full line). Since it was not possible to place the neutron source inside the vacuum vessel, additional measurements were performed with the neutron source at different poloidal positions. Fig. 1b contains the fitted data points corresponding to four poloidal positions of the neutron source around the vacuum vessel (curves marked with A,I,O,U). The data have been combined to one curve (dashed line), which should be representative for the neutron source placed on the torus axis. Again, the full line gives the dependence expected from a quadratic distance law.

In order to calculate the central ion temperature from the integral neutron flux measurements, the (measured) radial profile of the plasma density and the temporal evolution of the plasma parameters have been taken into account. An error of $le10\%$ can be caused by making assumptions about the shape of the ion temperature profiles The D^+-density was derived from the electron density measurements by corrections for Z_{eff} (measured from soft X-continuum radiation [4]) and for the estimated D^+/H^+ -ratio (D^+-plasma, H^0-injection).

The D-D maxwellian reactivities were calculated with a generalized Kozlov formula [5]. A first example for the analysis of the neutron flux data is presented in fig. 2. In this case the data of 9 similar discharges heated by 3 neutral beam injectors were averaged. The time evolution of the measured count-rate is plotted in fig. 2 a. The scale on the right gives the evaluated total neutron production rate of the plasma. Fig. 2b contains the ion temperature calculated from the neutron flux (crosses). Additionally the measured data from the CX- and the CXRS-diagnostics are given, which are in good agreement with the neutron data. The ion temperature generally exceeds the electron temperature during NBI, as indicated by the dashed line which gives T_e from the soft X filter method [4].

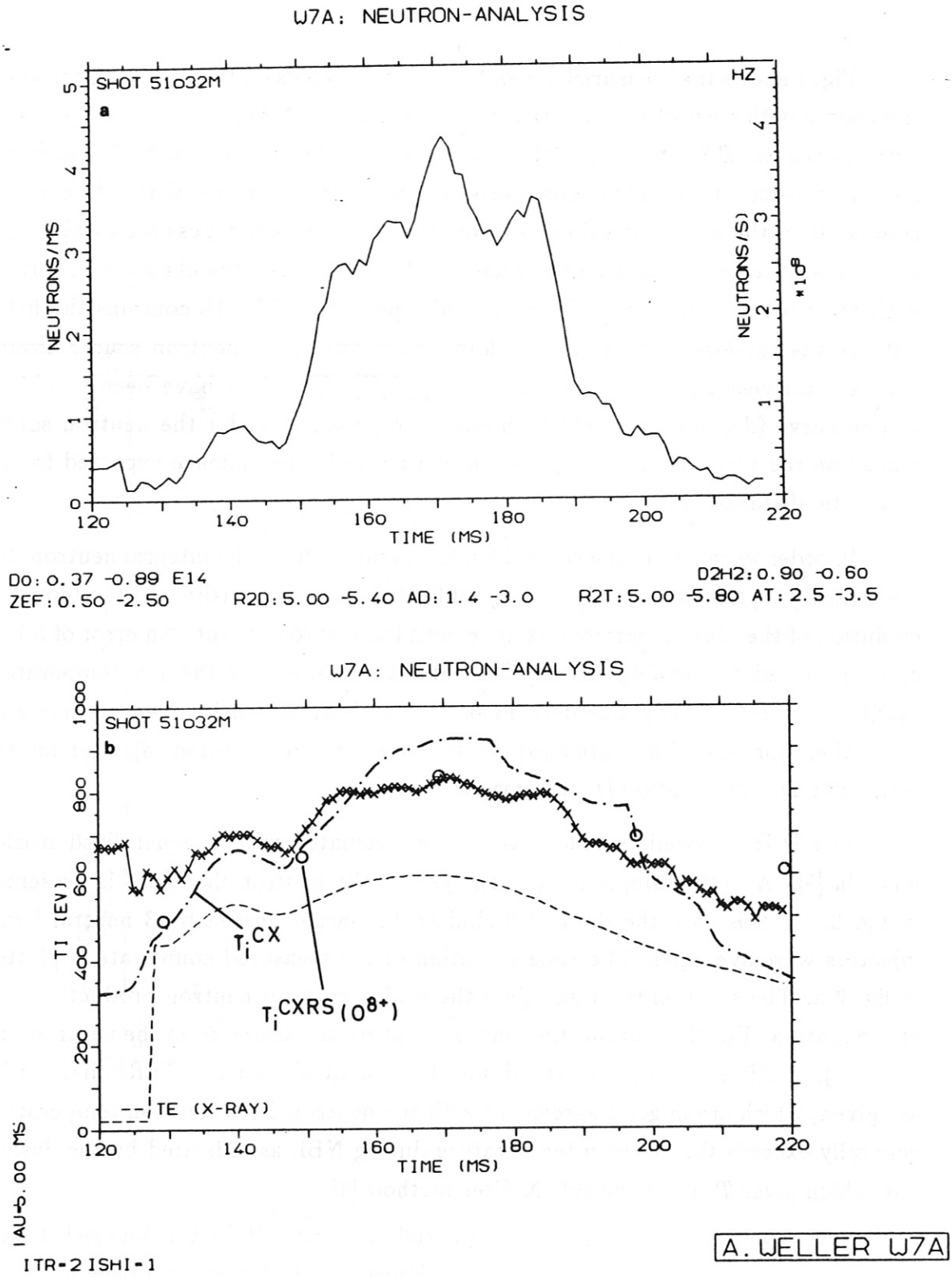

Fig. 2 a) Measured neutron flux during NBI (3 inj.).
b) Ion temperature evaluation from neutron flux compared with CX- and CXRS-data and electron temperature.

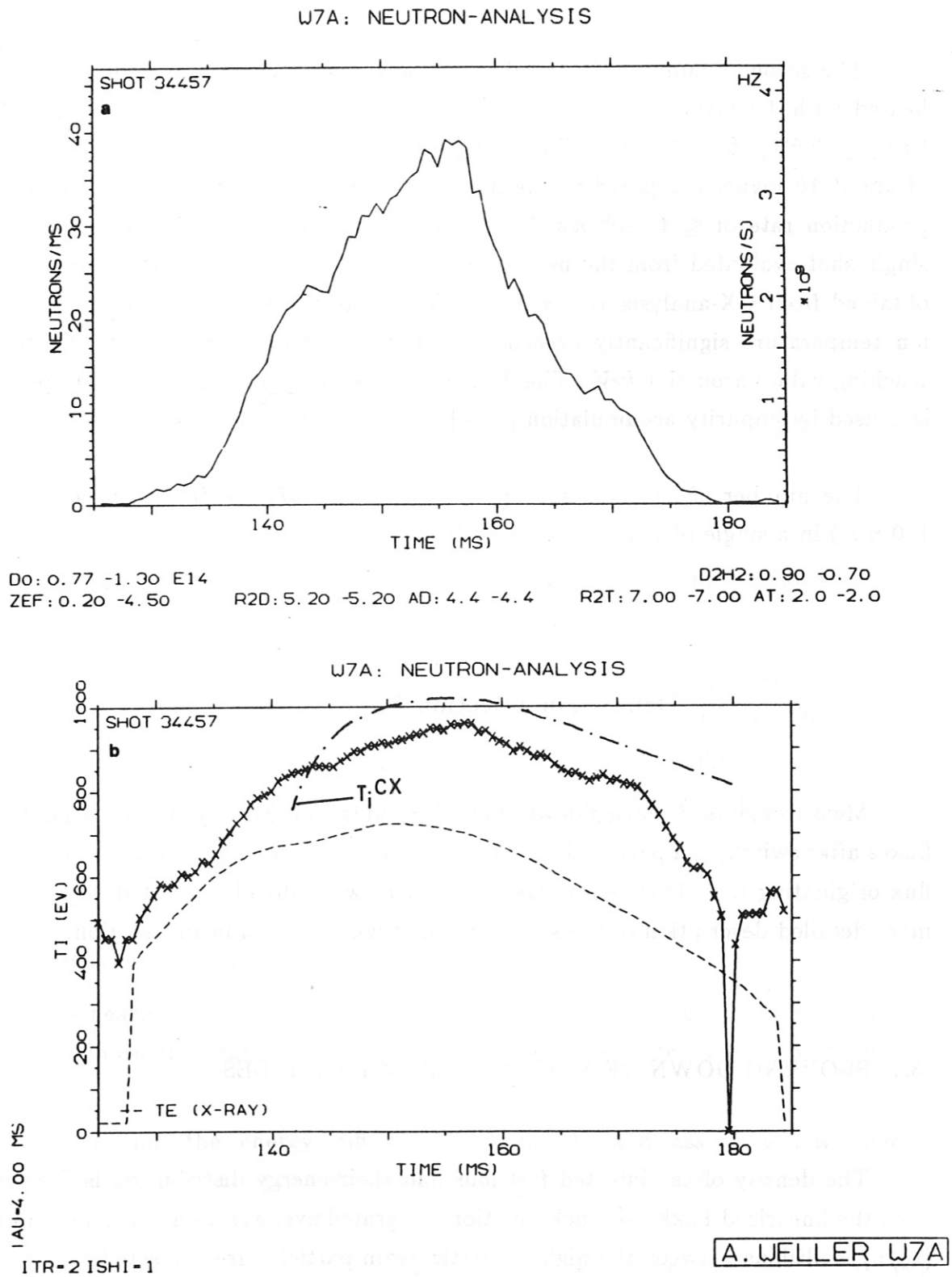

Fig. 3 a) Measured neutron flux during NBI (4 inj.).

b) Ion temperature evaluation from neutron flux compared with CX-data and electron temperature.

The second example refers to discharges with maximum achievable pressure, heated with 4 neutral beam injectors and density increase by D_2-pellet injection ($\beta(0) \leq 0.6\%$, $B = 3.2\ T$). The measured count-rate of $\leq 40\ kHz$ is a factor of about 10 higher compared to the first case and corresponds to a total neutron production rate of $\leq 4 \cdot 10^9\ n\,s^{-1}$ (fig. 3a). In fig. 3b the ion temperature of a single shot evaluated from the neutron flux (crosses) is compared with the results obtained from CX-analysis and with the electron temperature (dashed line). The ion temperature significantly exceeds the electron temperature [1,2] during NBI reaching values around 1 keV. The decrease of the temperatures in the late phase is caused by impurity accumulation [1,2,6].

The number of neutrons produced during NBI ($H^0 \rightarrow D^+$ -plasma, $\Delta t \leq 120\ ms$) in a single plasma shot is $\leq 1 \cdot 10^{10}$.

3. Neutron Flux during Deuterium Injection Experiments

Measurements of slowing down times derived from the decay of the CX-neutral fluxes after switching a part of the NBI power for a short time and from the neutron flux originating from D-D beam-plasma reactions were already reported in [2,7]. A more detailed description of the second method will be given in this section.

3.1. SLOWING DOWN OF NEUTRAL BEAM PARTICLES

The density of the injected fast ions and their energy distribution is derived from the linearized Fokker-Planck equation integrated over gyration angle and pitch ($v_\parallel / v$), collisions between the high energetic beam particles are neglected:

$$\frac{\partial f_b}{\partial t} = \frac{\Gamma_b}{v^2} \frac{\partial}{\partial v} \left(\alpha_1 f_b + \frac{1}{2} \frac{\partial}{\partial v} \alpha_2 f_b \right) + S_b^* - L_b^* \qquad (1)$$

with $\Gamma_b = \dfrac{\ln \Lambda}{4\pi} \left(\dfrac{Z_b e^2}{\epsilon_0 m_b} \right)^2$

$$\alpha_1 = -v^2 \frac{dh_b}{dv} - \frac{dg}{dv}$$

$$\alpha_2 = v^2 \frac{d^2 g}{dv^2}$$

$$S_b^* = \sum_{\nu=1}^{3} S_{b_\nu}^* \cdot \delta(v - v_\nu) \qquad \text{source term}$$

L_b^* : loss term (thermalization)

f_b : distribution function of fast beam injected ions

The subscript b refers to the beam injected particles where the additional subscript ν denotes particles injected with 1/1, 1/2 and 1/3 of the full energy (injection velocities v_ν). The quantities h_b and g are the Rosenbluth potentials for a Maxwellian background plasma. $S_{b_\nu}^*$ is related to the source strengths S_{b_ν} via:

$$\int_v^\infty v^2 \sum_\nu S_{b_\nu}^* \, \delta(v - v_\nu) \, dv = \sum_\nu S_{b_\nu} \cdot \Theta(v_\nu - v)$$

where Θ is the step function.

As nearly all neutrons are produced by the high energy component of the slowing down distribution, the estimation of f_b is restricted to the high energy range.

Neglecting the energy diffusion term in (1) and assuming low energy Maxwellian background ($v_{th_i} \ll v \ll v_{th_e}$; $v_{th_\alpha}^2 = \frac{2T_\alpha}{m_\alpha}$ $(\alpha = i, e)$) yields:

$$\frac{\partial f_b}{\partial t} = \frac{\Gamma_b}{v^2} \frac{\partial}{\partial v} \left((\alpha_e v^3 + \alpha_i) f_b \right) + S_b^* - L_b^* \qquad (2)$$

with $\alpha_e = \dfrac{4}{3\sqrt{\pi}} n_e \dfrac{m_b}{m_e} \dfrac{1}{v_{th_e}^3}$

$$\alpha_i = Z_i^2 \, n_i \frac{m_b}{m_i}$$

The characteristic system of the 1st order differential equation (2) is:

$$d\,t \cdot \left(\alpha_e v^3 + \alpha_i\right) = -\frac{v^2}{\Gamma_b}\, d\,v = \frac{d\,F_b}{S_b^* - L_b^*}$$

where

$$F_b = \left(\alpha_e\, v^3 + \alpha_i\right) f_b$$

Integration yields:

$$t - t_0 = \tau_c \,\ln \frac{\alpha_e\, v_0^3 + \alpha_i}{\alpha_e\, v^3 + \alpha_i} \qquad \text{with} \quad \tau_c = \frac{1}{3\alpha_e\, \Gamma_b}$$

$$F_b - F_{b_0} = -\frac{1}{\Gamma_b} \int_{v_0}^{v} v^2\, (S_b^* - L_b^*)\, d\,v$$

The slowing down time t_{sd} is defined as the time the beam particles need until their initial velocity $v_0 = v(t_0) = v_{NI}$ is reduced to the thermal velocity ($v(t_{sd}) \sim v_{th_b}$). With

$$v_{th_b} \ll \left(\frac{\alpha_i}{\alpha_e}\right)^{\frac{1}{3}}$$

follows for the slowing down time:

$$t_{sd} \approx \tau_c \,\ln\!\left(1 + \frac{\alpha_e}{\alpha_i} v_{NI}^3\right) \tag{3}$$

Then the **stationary slowing down distribution** can be estimated assuming

$$v_0 \to \infty \quad ; \quad F_{b_0} \to 0$$

and

$$L_b^* = 0 \quad \text{for} \quad \mathrm{v} \gg \mathrm{v_{th_i}} \qquad \text{(only thermalized particles are lost)}$$

This leads to

$$f_b(v) = \frac{1}{\left(\alpha_e v^3 + \alpha_i\right) \Gamma_b} \sum_{\nu} S_{b_\nu} \cdot \Theta(v_\nu - v) \tag{4}$$

The **transient** behaviour of the slowing down distribution after switching off the source at $t = 0$ ($S_b^* = 0$ for $t > 0$) is calculated with the initial value of the stationary solution:

$$F_b(t = 0) \equiv F_{b_0} = \frac{1}{\Gamma_b} \sum_{\nu} S_{b_\nu} \cdot \Theta(v_\nu - v_0)$$

with

$$v_0 \equiv v_0(v,t) = \left((v^3 + \frac{\alpha_i}{\alpha_e}) e^{t/\tau_c} - \frac{\alpha_i}{\alpha_e} \right)^{\frac{1}{3}}$$

resulting in the **time dependent solution:**

$$f_b(v,t) = \frac{1}{(\alpha_e v^3 + \alpha_i)\,\Gamma_b} \sum_{\nu} S_{b_\nu} \cdot \Theta(v_\nu - v_0(v,t)) \tag{5}$$

The **neutron production rate** from D-D beam-plasma reactions R_{DD} can be expressed by

$$R_{DD} = \int_{v_{th_b}}^{\infty} n_D^{th} \cdot f_b(v)\, v^2 \cdot \sigma(v)\, v\, d\, v \tag{6}$$

where n_D^{th} is the thermal background D^+-density, σ is the D-D fusion cross section (neutron branch), and f_b is given by eq. (4). The cross section σ is calculated with the Duane coefficients [8].

3.2. EXPERIMENTAL RESULTS

In most of the experiments D^0 was injected only with one additional neutral beam line switched on for $\sim$ 20 ms. The target plasma was started in D_2 as usual and heated by three neutral beam lines injecting H^0. As in the case of the thermal neutron production the D^+-density was derived from the electron density measurements by corrections for Z_{eff} and for the D^+/H^+ -ratio.

For the calculation of the absolute values of the neutron flux, the plasma parameters were approximated by homogeneous values inside a radius of 5 cm. The neutron production outside this hot plasma region was neglected. The additional error introduced by this procedure should be negligible compared with the uncertainity of a factor $\sim$ 2 which is expected anyhow for the measured neutron flux.

The number of injected deuterium particles was derived from the measured injection beam power and the fractional abundance of 0.21 : 0.32 : 0.47 for particles with $E = \frac{1}{1} : \frac{1}{2} : \frac{1}{3}$ of the full energy (27 keV) according to earlier measurements [9]. Because of the relatively high shine-through losses [1] of $\sim 0.5 - 0.2$ of the injected particles, corrections for this effect were applied.

In addition to the standard ^3He-detector, which had a fixed position and served as a reference monitor, a second detector of same type and a NE-213 liquid scintillator detector were installed. These detectors could be moved in a restricted range around the machine, in order to investigate the toroidal distribution of the fast particles injected in one particular toroidal plane. The liquid scintillator detector equipped with fast electronics also served to inspect the signals of the ^3He-detectors for count-losses because the neutron fluxes due to beam-plasma interaction exceed the fluxes generated from thermal plasma ion interaction by a factor of ~ 20. In fig. 4 signals of a ^3He-counter (fig. 4a) and of the NE-213 liquid scintillator detector are compared during NBI with all the three beam lines operated with D^0. The dip in the signals after $\sim 180\ ms$ generated by a short interuption of one of the injectors is less in the first case owing to count losses of the ^3He-counter above count rates of $\sim 400 - 500\ kHz$.

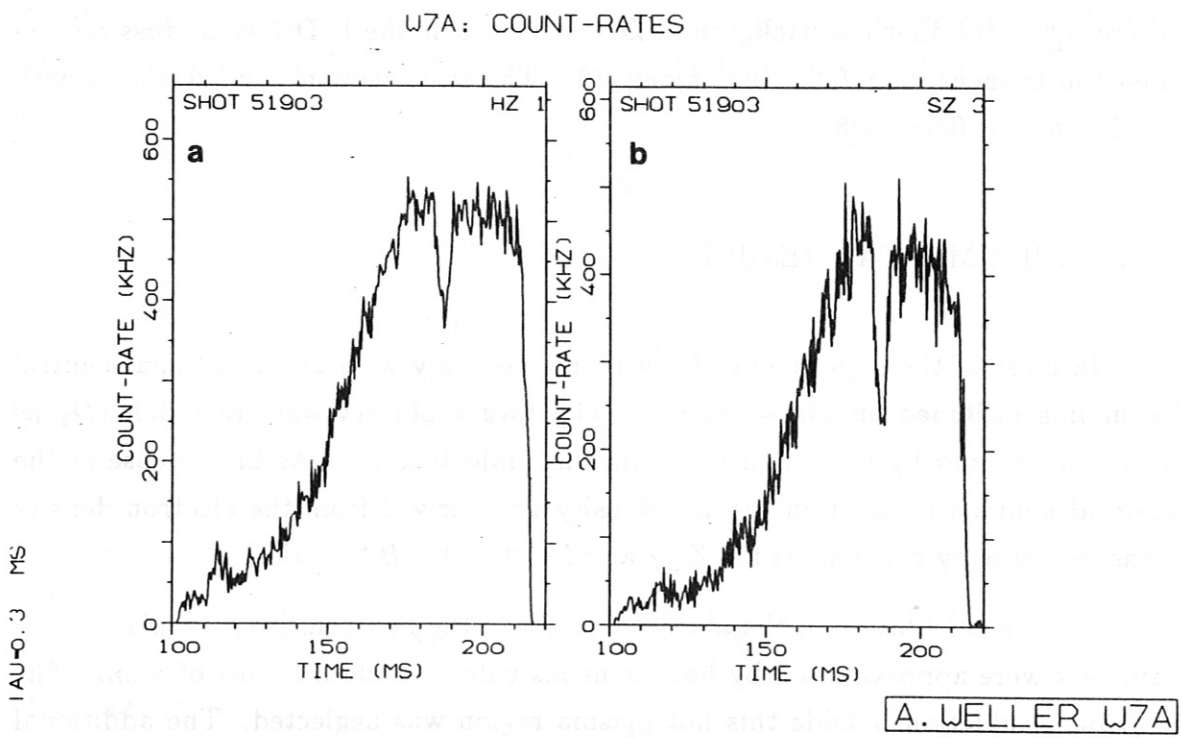

Fig. 4 Neutron flux signals during D^0-injection (3 inj.).
a) Signal from ^3He-counter.
b) Signal from NE-213 detector.

With respect to the toroidal distribution of the neutron production rate no evidence of asymmetries was found apart from an enhancement by a factor of ~ 2 at the place of injection. This results from the interaction of the injected deuterium, not

absorbed by the plasma, with deuterium adsorbed on the beam dump plate. At the injection port, this fraction is comparable with the neutron flux from beam-plasma reactions. But this local production does not interfere with the measurements made in some distance away from the D^0-injector as derived from operating the injector without target plasma.

The toroidal symmetry of the neutron production means, that the characteristic time for the slowing down of the fast ions is long compared with the transit time of these ions around the torus. This result also justifies the neutron flux calculations, which are based on the assumption of a uniform toroidal distribution of the densities.

The neutron production at the beam dump plates also gives informations about the fraction of the injected particles which are absorbed by the plasma. This can be derived from injection into the plasma and into the empty torus resulting in almost equal signals. Together with the measurements made far away from the injection port, an absorption consistent with the values expected from beam deposition calculations is derived.

The neutron flux obtained without target plasma also provides a monitor signal which gives the transient time response of the D^0-injection source after switching on/off the injector. Fig. 5a shows a neutron flux signal from the injection port without target plasma during injector switch off. The decay time of $< 0.4\ ms$ is much less compared with signal decay times from beam plasma interaction.

Fig. 5b contains the time behaviour during injection into a target plasma observed with the reference neutron counter, which does not detect any signal without plasma. This justifies the assumption of a step function in time for the source term leading to the time dependent solution given in eq. (6). The dashed line in fig. 5b already represents the calculated neutron signal according to the model introduced in section 3. 1. The calculated signal is normalized in amplitude to the experimental curve. The absolute values (without normalization) differ by a factor of ~ 2, which is rather satisfactory with respect to all the experimental uncertainities of measuring absolute neutron fluxes and of the plasma parameters used in the calculations.

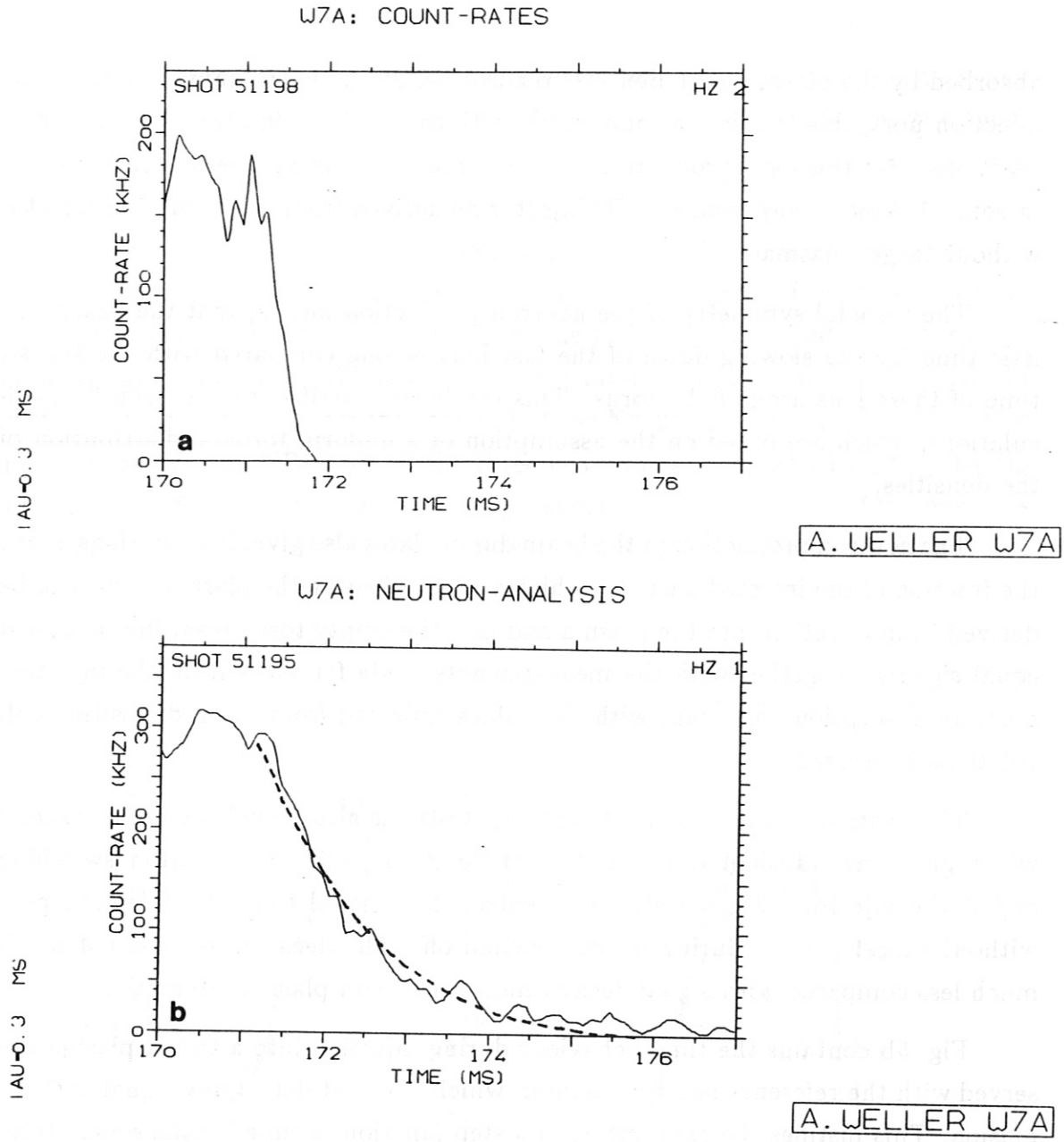

Fig. 5 Neutron flux signals during switch off the D^0-injector.

a) Signal at injection port without plasma.

b) Signal from beam plasma $D - D$ reactions (detector far away from injection port).

In order to correlate the neutron signals (absolute values during the stationary phase and decay times after switch off of the injector) with the calculated slowing down for different plasma parameters, the D^0-injection was shifted in time corresponding to changes of the plasma density and temperature.

The following sequence of figures (figs. 6,7,8) summarizes the results obtained from additionally operating a D^0-injector at three different times.

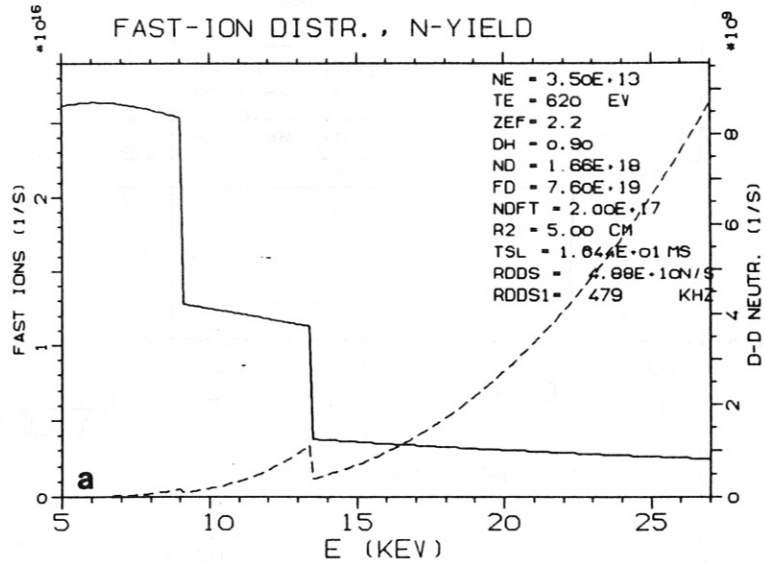

A. WELLER W7A

W7A: NEUTRON-ANALYSIS

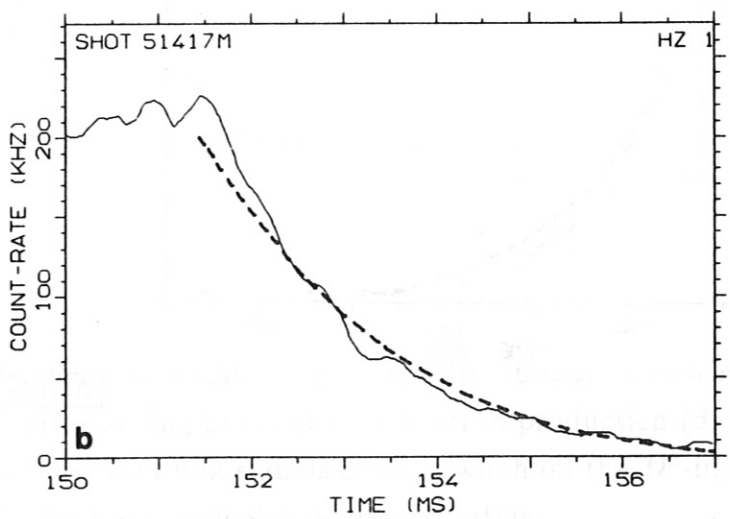

A. WELLER W7A

Fig. 6 a) Calculated stationary energy distribution of slowing down particles and corresponding beam-plasma neutron production (dashed line).
b) Neutron flux signals during switch off the D^0-injector at $\sim 151.5\ ms$. Dashed line: calculated time evolution.

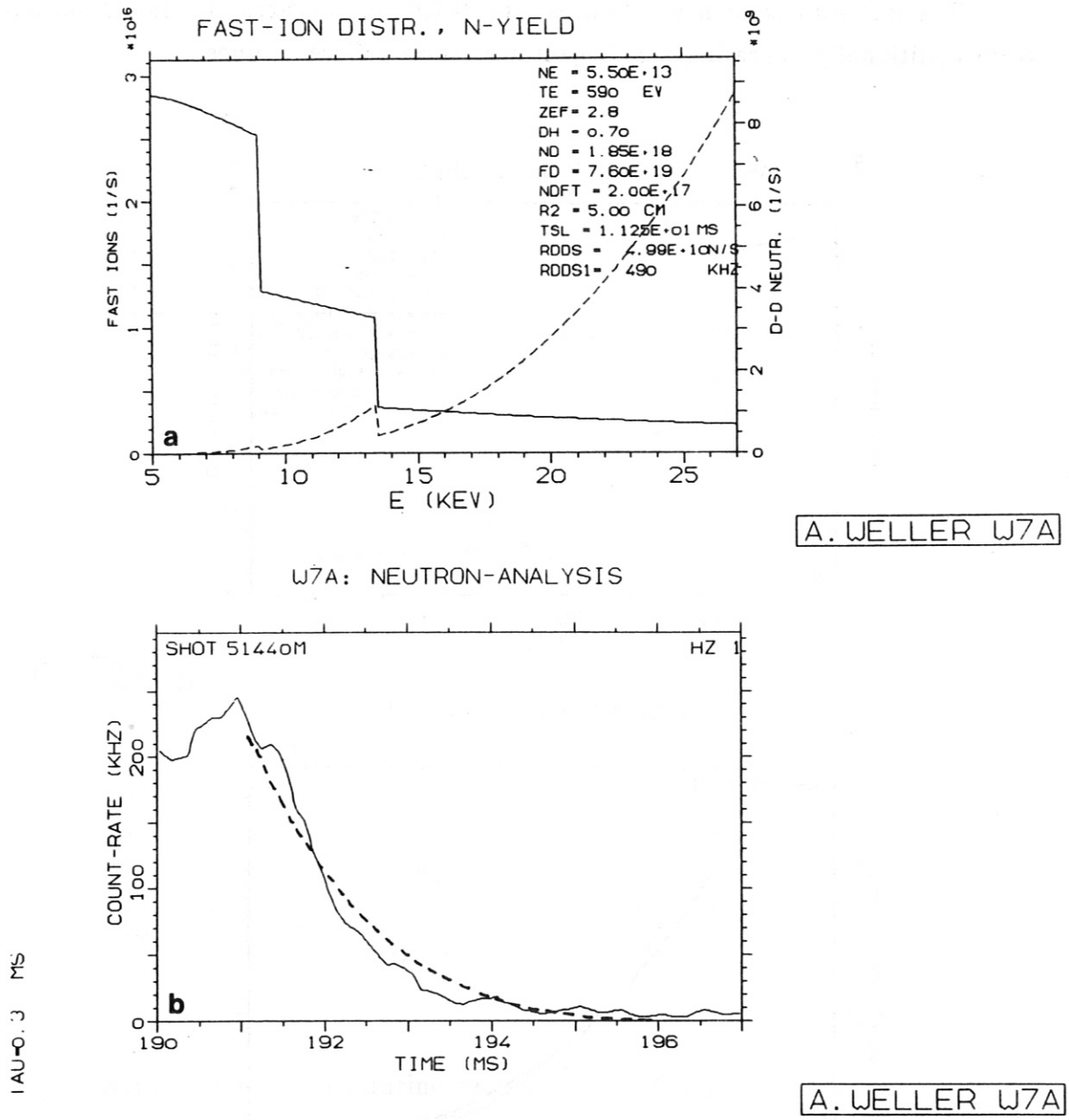

Fig. 7 a) Calculated stationary energy distribution of slowing down particles and corresponding beam-plasma neutron production (dashed line).
b) Neutron flux signals during switch off the D^0-injector at $\sim 191.0\ ms$. Dashed line: calculated time evolution.

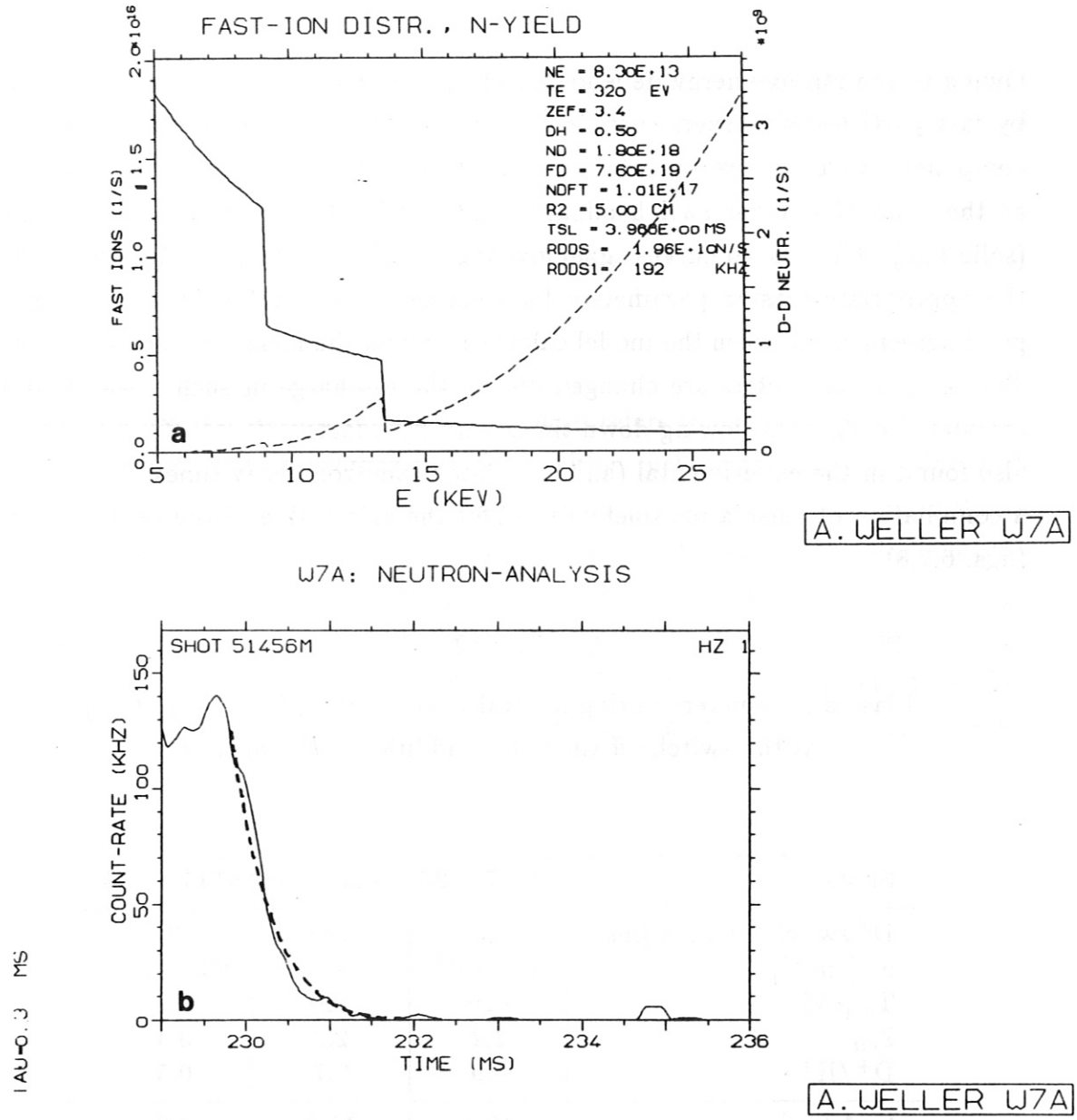

Fig. 8 a) Calculated stationary energy distribution of slowing down particles and corresponding beam-plasma neutron production (dashed line).
b) Neutron flux signals during switch off the D^0-injector at $\sim 227.0\ ms$. Dashed line: calculated time evolution.

In the upper part of each figure the calculated stationary energy distribution of the slowing down particles $f_b(v)\,v^2$, according to eq. (4) is plotted (full line) as a function of the particle energy ($v^2 = \frac{2E}{m_D}$). The steps in the function correspond to the sources at the three particular energies. In addition, the dashed line gives the corresponding distribution of the neutron production rate (integrand of eq. (6)).

Owing to the strong energy dependence of σ, nearly all the neutrons are produced by fast particles with energies $E \geq 15\ keV$, which originate from the full energy component with the lowest particle fractional abundance. The neutron flux signals at the time of injector switch off are displayed in the lower part of the figures (solid line). The dashed curves again give the calculated signals (normalized) taking the appropriate plasma parameters for each case. As for the first case (fig. 5b) good agreement between the model calculations and the measurements is obtained. The plasma parameters are changed during the discharge in such a way that the calculated collisional slowing down times vary by a factor of ~ 4. This variation is also found in the experimental (and calculated) neutron decay times. Table I gives a compilation of plasma parameters used for the calculation of the neutron signals (figs. 6,7,8).

Table I

Plasma parameters during neutral beam heating (3 H^0-injectors) at the switch off time of an additional D^0-injector

Shots	51417 – 27	51440 – 43	51456 – 59
D^0 switch off time [ms]	150	190	230
n_e [cm^{-3}]	$3.5 \cdot 10^{13}$	$5.5 \cdot 10^{13}$	$8.3 \cdot 10^{13}$
T_e [eV]	620	590	320
Z_{eff}	2.2	2.8	3.4
D^+/H^+	0.9	0.7	0.5
t_{sd} * [ms]	16.4	11.3	4.0
stat. neutron flux [s^{-1}]			
calculated :	$4.9 \cdot 10^{10}$	$5.0 \cdot 10^{10}$	$2.0 \cdot 10^{10}$
measured :	$2.2 \cdot 10^{10}$	$2.3 \cdot 10^{10}$	$1.3 \cdot 10^{10}$

* calculated slowing down time $27 \rightarrow 5\ keV$.

Also included are the stationary values of the experimentally observed and calculated neutron fluxes from beam-plasma reactions. These values also agree within a factor of ~ 2. The relative change of the experimental stationary fluxes corresponds to the variation expected from the calculations. The decrease of the slowing down times from $\sim 16\ ms$ to $\sim 4\ ms$ leads to a an enhancement of the low energy components in the stationary slowing down distributions as can be deduced from comparing figs. 6a,8a.

Finally the last example presented in fig. 9 refers to an experiment where the D^0-injection occurred at another toroidal position just on the opposite side with respect to the standard neutron detector (in the original case the toroidal distance between D^0-injector and detector was much smaller). The dashed curves gives the time behaviour calculated with the given plasma and injection parameters. The absolute neutron fluxes in the calculation are again about twice the experimental values. This result confirms the toroidal symmetry of the neutron production. The signal of the NE-213 detector shown in fig. 9b agrees well with the ^3He-counter signal, indicating negligible count losses.

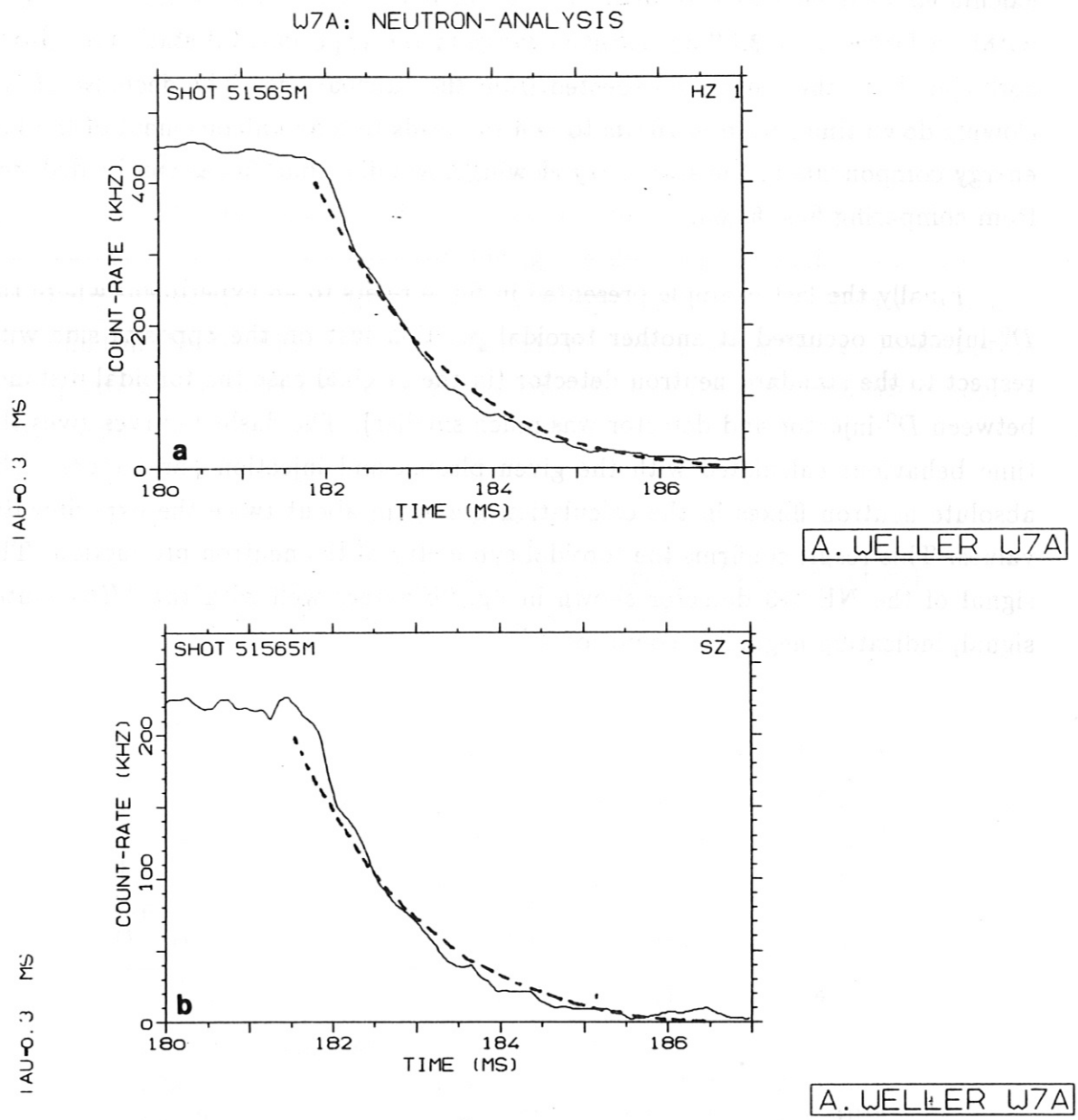

Fig. 9 Neutron flux signals during D^0-injection at another toroidal position. Dashed line: calculation.

a) Signal from ^3He-counter.

b) Signal from NE-213 detector.

4. Summary

The evaluation of the ion temperature from the neutron flux which is produced by $D-D$ plasma ion fusion reactions generally leads to good agreement with the results of other measurements (CX-analysis, CXRS). The method is limited to plasmas with $T_i > 500\ eV$, $n_e > 5 \cdot 10^{13}\ cm^{-3}$. Although many plasma parameters have to be known as input for the calculation of the temperature and errors of the absolute flux measurements in the order of $\sim 30\%$ may occur, the error propagation for T_i is rather moderate owing to the strong dependence of the $D-D$ cross section on the temperature. Thermal neutron production rates of $\leq 4 \cdot 10^9\ neutrons\ s^{-1}$ have been measured in Wendelstein VII-A for plasmas with T_i close to $1\ keV$.

Time resolved neutron flux measurements yield informations about the slowing down of the injected particles and thus on the heating mechanism of NBI with D^0. The results have been derived from the neutron reactions between fast D^+-ions resulting from injection and the thermal D^+ ions of the bulk plasma, in particular from:

- the toroidal distribution of the neutron production rate (source of fast particles located at a particular toroidal position). Note that full energy particles need $\sim 0.035\ ms$ to travel around the torus. This is about two orders of magnitude shorter compared with the collisional slowing down times.
- the stationary neutron flux during D^0-injection.
- the transient behaviour of the neutron flux during switch on/off the D^0-injector.

The experiments show symmetric distributions of the neutron production along the toroidal direction. This would not be expected in the case of very fast, non-collisional slowing down of the injected ions. The agreement between experiment and calculations based on a collisional slowing down model is rather good in all the cases investigated. Therefore, classial collisional slowing down of injected beam neutrals seems to be obvious in the WVII-A stellarator.

Acknowledgements

The experimental investigations were a common effort of the whole WVII-A team. In particular, the authors would like to thank Dr. M. Kick, Dr. J. Junker, Dr. W. Ohlendorf and Dr. H. Ringler for providing the CX- and CXR-data.

References

[1] W VII-A TEAM, NI GROUP, Proc. 9th Int. Conf. on Plasma Physics and Controlled Nuclear Fusion Research, Baltimore 1982, Nucl. Fusion Suppl., Vol. 2, (1983) 241

[2] W VII-A TEAM, NI GROUP, Proc. 10th Int. Conf. on Plasma Physics and Controlled Nuclear Fusion Research, London 1984, Nucl. Fusion Suppl., Vol. 2, (1985) 371

[3] ASSI, G., RAPP, H., A Neutron Flux Measurement system for ASDEX, Max-Planck-Institut für Plasmaphysik Garching, Rep. IPP 3/70 (1981).

[4] SMEULDERS, P., Soft X-ray fluxes as a diagnostic for hot plasmas, Max-Planck-Institut für Plasmaphysik Garching, Rep. IPP 2/233 (1979).

[5] HIVELEY, L.M., Nuclear Fusion 17 (1985) 873

[6] W VII-A TEAM, NI GROUP, Nuclear Fusion 25 No. 11 (1985)

[7] W VII-A TEAM, NI GROUP, 5th Intern. Workshop on Stellarators, (Proc. of the IAEA Technical Committee Meeting on Plasma Confinement and Heating in Stellarators, Schloss Ringberg (FRG), 1984), Vol. 1, CEC, Brussels (1984) 179.

[8] DUANE, B.H., Fusion Cross Section Theory, Battelle Pacific Northwest Labs, Report BNWL-1685 (November 1972).

[9] OTT, W., FREUDENBERGER, K., PENNINGSFELD, F.P., PROBST, F., SÜSS, R., Rev. Sci. Instrum. 54 (1983) 50